Digital discrimination of neutrons and γ rays with organic scintillation detectors in an 8-bit sampling system using frequency gradient analysis*

YANG Jun(杨俊) LUO Xiao-Liang(罗晓亮)[1)] LIU Guo-Fu(刘国福) LIN Cun-Bao(林存宝)
WANG Yan-Ling(王艳玲) HU Qing-Qing(胡青青) PENG Jin-Xian(彭进先)

Department of Instrument Science and Technology, National University of Defense Technology, Changsha 410073, China

Abstract: The feasibility of using frequency gradient analysis (FGA), a digital method based on Fourier transform, to discriminate neutrons and γ rays in the environment of an 8-bit sampling system has been investigated. The performances of most pulse shape discrimination methods in a scintillation detection system using the time-domain features of the photomultiplier tube anode signal will be lower or non-effective in this low resolution sampling system. However, the FGA method using the frequency-domain features of the anode signal exhibits a strong insensitivity to noise and can be used to discriminate neutrons and γ rays in the above sampling system. A detailed study of the quality of the FGA method in BC501A liquid scintillators is presented using a 5 G samples/s 8-bit oscilloscope and a 14.1 MeV neutron generator. A comparison of the discrimination results of the time-of-flight and conventional charge comparison (CC) methods proves the applicability of this technique. Moreover, FGA has the potential to be implemented in current embedded electronics systems to provide real-time discrimination in standalone instruments.

Key words: n-γ discrimination, liquid scintillator, FGA, 8-bit sampling system

PACS: 29.30.Hs, 29.40.Mc, 28.41.Rc **DOI:** 10.1088/1674-1137/36/6/011

1 Introduction

Organic scintillation detectors have often been used for the detection and spectroscopy of a wide assortment of radiations. When they are used as neutron detectors, pulse shape discrimination (PSD) is an essential requirement because all neutron fields coexist with an associated γ-ray component, arising as a result of scattering reactions of the neutrons with materials in the environment and as direct by-products of the primary reaction producing neutron field [1].

A number of techniques for PSD have been investigated with varying degrees of success. The most popular ones of these are the charge comparison method [2, 3] and the zero crossing method [4, 5]. Both of these methods were originally implemented in analogue electronics, often in dedicated instrumentation modules or nuclear instrument modules (NIMs). More recently, both of these methods have been implemented in the digital domain as digital electronic platforms have become available with the requisite speed and cost to make this possible [6–8]. These methods have become the industrial standards used for comparisons with other new proposed discrimination methods, such as the correlation method [9], the curve-fitting method [10], the pulse gradient analysis (PGA) method [11–13], the artificial neural networks method [14], the fuzzy c-means algorithm [15], the wavelet algorithm [16, 17], the FGA method [18], and so on. Additionally, some discrimination approaches, such as PGA and FGA, can provide real-time, digital characterization of environments where neutrons and γ rays coexist.

However, in order to obtain a satisfactory discrimination quality, most of the above-mentioned algorithms require high performance digital electronic

Received 8 October 2011
* Supported by National Natural Science Foundation of China (A050508/11175254)
1) E-mail: delongtmac@163.com

platforms. Generally speaking, the bit resolution of the ADC in the sampling system should be at least 12-bit [19]. As the 8-bit ADC is cheaper and easier to use than the 12-bit ADC, for example, the price of the 500 M samples/s 8-bit AD9284 is less than half that of the 500 M samples/s 12-bit AD9434 [20], it is valuable to study the feasibility and the applicability of the algorithms mentioned above in an 8-bit sampling platform.

Most of the above pulse shape discrimination methods use the time-domain features of the signal, e.g., the implementation of the PGA method is based on a comparison of the relative heights of samples in the trailing edge of the pulse. Since the scintillation process and the photomultiplier tube (PMT) anode signal are often very noisy and time-domain features are naturally highly dependent on the signal amplitude at a specific time, these pulse shape discrimination methods can have a great dependency on the de-noising algorithm. In contrast, the discrimination methods developed in frequency-domain, such as the wavelet method and FGA method, are more robust to noise and abrupt changes in the pulse waveform. But the calculation overhead of the wavelet-based PSD method is heavier than that of the FGA algorithm and thus it is not suitable for real-time discrimination. The FGA method exploits the difference between the zero-frequency component and the first frequency component of the Fourier transform of the acquired signal and combines the advantage of insensitivity to noise associated with spectral analysis with that of the real-time implementation of the PGA algorithm.

According to the above considerations, we will compare the feasibility and the performance between the CC method and the FGA method in an 8-bit sampling platform in this paper. The comparison will proceed in two aspects as follows.

(1) Verification of the CC and FGA by the time-of-flight (TOF) method. Since the TOF is a high-accuracy method of n-γ discrimination in most circumstances, the result of the TOF will be used as the basic criterion for comparing the feasibility of CC and FGA in the environment of an 8-bit sampling system. If either of these two methods' results differs strongly from the TOF, then this method is deemed to be no longer feasible under this low bit resolution condition.

(2) Performance comparison of CC and FGA. The FOM of each method will be obtained and compared. A larger value of FOM indicates better performance of the n-γ discrimination method.

An experimental environment has been constructed mainly with an associated particle neutron generator, a TOF measurement system and a 5 G samples/s 8-bit digital capture oscilloscope. The detailed description of this experimental environment is given in Section 2; the experimental results and the discussion are given in Section 3; the conclusions arising from this research are given in Section 4.

2 The experiment

The experimental data analyzed in this work were acquired using the TOF measurement system at the Institute of Nuclear Physics and Chemistry, the Chinese Academy of Engineering Physics, Mianyang, China. As shown in Fig. 1, through deuterium-tritium fusion reaction, which is accomplished by using a 1 μA deuterium beam whose average energy is 110 keV to bombard the tritium target in this experiment, an associated particle neutron generator (APNG) produces neutrons and alpha particles that are correlated in time and travel in opposite directions to conserve momentum. The energies of neutrons and alpha particles are 14.1 MeV and 3.5 MeV, respectively.

For TOF research, one plastic scintillation detector detects the arrival of the alpha particle beam pulse and provides a timing reference point for the arrival of each pulse and is referred to as the beam-pickup signal, and the other liquid scintillation detector placed at an adjustable distance from the tritiated target detects the corresponding neutrons or γ rays. The plastic scintillation detector consisted of a Φ25.4 mm × 0.1 mm cylindrical cell scintillation detector, optically coupled to an EMI 9807B PMT, which was operated with a negative supply voltage of −1600 V DC. The output signal from the plastic scintillator was connected to Channel 1 of a Tektronic digital phosphor oscilloscope, via approximately 25 m of high bandwidth cable. The liquid scintillation detector consisted of a Φ50.8 mm × 50.8 mm cylindrical cell scintillation detector filled with BC501A organic liquid, optically coupled to another EMI 9807B PMT, which was operated with a negative supply voltage of −1400 V DC. The output signal from the liquid scintillator was connected to another input of the digital oscilloscope and used to trigger acquisition.

The liquid scintillator pulse and the corresponding beam-pickup pulse data were captured digitally with a sampling rate of 5 G samples/s and 8-bit amplitude resolution. This enabled all detected events, i.e. both γ rays and neutrons, to be sorted in terms

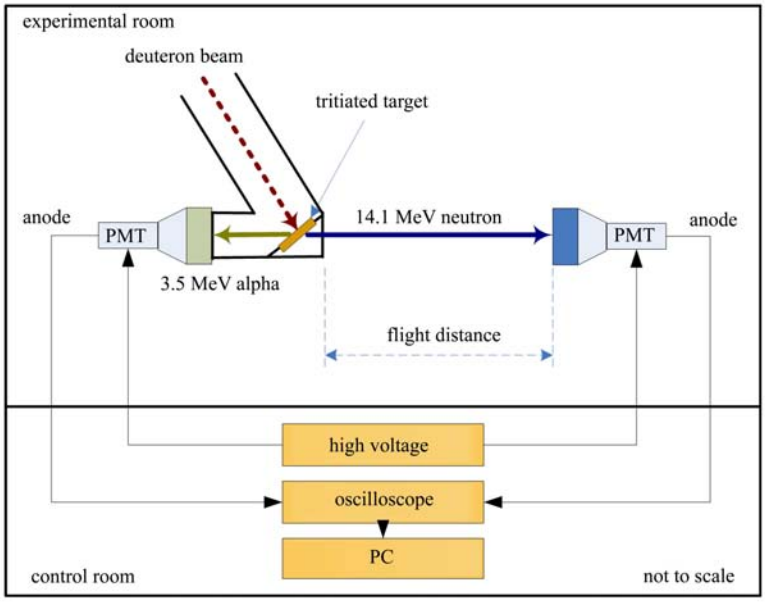

Fig. 1. A schematic of the experimental set-up used for the associated particle neutron generator at the Institute of Nuclear Physics and Chemistry, the Chinese Academy of Engineering Physics, Mianyang, China.

of their time-of-arrival relative to the initial beam-pick up.

3 Results and discussion

3.1 Verification of FGA and CC by TOF

3.1.1 The TOF measurement

TOF measurement, based on the difference in flight time for neutrons and γ rays across a known flight path length, is a reliable means of discriminating neutron and γ-ray events. Hence it offers an effective way to verify different n-γ discrimination methods and to measure the degree of discrimination quality on a quantitative basis [21].

In our research, the distance between the liquid scintillation detector and the tritiated target, i.e., the flight path length, was set as 1500 mm. A total of 1411 events were recorded and analyzed. The results of the TOF method are given in Table 1. $N_{\text{n-TOF}}$ and $N_{\gamma\text{-TOF}}$ represent the number of neutron and γ-ray events discriminated by TOF, respectively.

According to Table 1, 774 events are identified as 20 γ-ray events and 754 neutron events, but the other 637 events can not be discriminated and can only be classified as scatter events, which arise as a result of scatter in the environment and within the detector. These scatter events can be either γ-ray events or neutron events. However, the TOF method failed to classify them in terms of their radiation types. The reason for this invalidation of the TOF method is that a reference point in time which is usually required in the TOF method is unavailable for scatter events.

The total 774 pulses induced by these events were also applied to the FGA and CC methods to verify the feasibility of each method respectively. The discrimination results of the CC and FGA methods are also shown in Table 1. $N_{\text{n-(TOF+FGA)}}$ is the number of neutron events correctly discriminated by FGA out of the 754 neutrons pre-identified by TOF and $N_{\gamma\text{-(TOF+FGA)}}$ is the number of γ-ray events correctly discriminated by FGA out of the 20 γ-ray pulses pre-identified by using the TOF method. For the CC method, $N_{\text{n-(TOF+CC)}}$ and $N_{\gamma\text{-(TOF+CC)}}$ are defined correspondingly. The corresponding calculation process will be given in the following para-graphs.

3.1.2 Frequency gradient analysis

Having discovered that there are distinct differences between the frequency spectrum of the γ-ray signal and the neutron signal, which can be used as prominent features to discriminate them, G. Liu et al. presented a novel n-γ discrimination method called FGA in paper [10]. It is demonstrated that the value of the Fourier transform of a neutron or γ-ray signal at zero frequency, $|X(0)|$, which is the average value of the signal, is the most distinct part between them. This can be explained by the fact that the falling portion of neutron pulse decreases more slowly than that of γ-ray events, which results in a greater average value of neutrons, $|X_{\text{n}}(0)|$, than that of γ-ray

Table 1. The discrimination results of TOF, FGA and CC.

result	TOF	FGA	CC
number of neutrons	754 ($N_{\text{n-TOF}}$)	743 ($N_{\text{n-(TOF+FGA)}}$)	735 ($N_{\text{n-(TOF+CC)}}$)
error	—	0.015	0.025
number of γ-rays	20 ($N_{\gamma\text{-TOF}}$)	19 ($N_{\gamma\text{-(TOF+FGA)}}$)	17 ($N_{\gamma\text{-(TOF+CC)}}$)
error	—	0.050	0.150

events, $|X_\gamma(0)|$, in the same time interval as expected intuitively. In order to decrease the noise and take full advantage of the information provided by the Fourier transform, the gradient analysis method is used to optimize the single parameter $|X(0)|$. The discrimination parameter is for this purpose defined as:

$$k(f)=\frac{|X(0)|-|X(f)|}{f}, \tag{1}$$

where $|X(f)|$ is the magnitude spectrum of the neutron or γ-ray signal at frequency f.

Traditionally, the quality of an n-γ discrimination method is often assessed qualitatively by plotting the amplitude of a given pulse against a parameter that is proportional to its decay rate. The resulting scatter plot exhibits two separate components if the discrimination of events in a field comprising both neutrons and γ rays is successful. In the context of the FGA method in this research, we selected the difference between the zero-frequency component and the first frequency component of the Fourier transform of the acquired signal, i.e. $|X(0)|-|X(1)|$, as the discrimination parameter to differentiate the neutron event from the γ-ray event.

The 754 neutron pulses and 20 γ-ray pulses pre-identified by the TOF method were applied to the FGA method and the scatter plot of the FGA method is shown in Fig. 2. As can be seen in Fig. 2, each γ-ray or neutron event has been denoted by a symbol corresponding to its TOF assignment, and two distinct groups of events were observed, each of which corresponds to the γ-ray and neutron events. According to the principle of FGA method, it is understandable that neutron events have a larger discrimination parameters. Therefore, the right group of events is identified as neutrons and the left group of events is regarded as γ rays by the FGA method. As expected, most of the γ-ray events are located in the left region of the scatter plot, while only one γ-ray event mistakenly classified by the FGA method is located in the right region. It was in this way that the number of γ-ray events derived from the FGA method, $N_{\gamma\text{-(TOF+FGA)}}$, was obtained as 19. Similarly, the number of neutron events derived from the FGA method, $N_{\text{n-(TOF+FGA)}}$, was gained. Thus the error of FGA in discriminating neutrons can be defined as:

$$\text{Error}=\frac{|N_{\text{n-(TOF+FGA)}}-N_{\text{n-TOF}}|}{N_{\text{n-TOF}}}. \tag{2}$$

Likewise, the error of FGA in discriminating γ rays and the error of CC in discriminating neutrons or γ rays can be calculated in this way. The discrimination results of FGA are shown in Table 1.

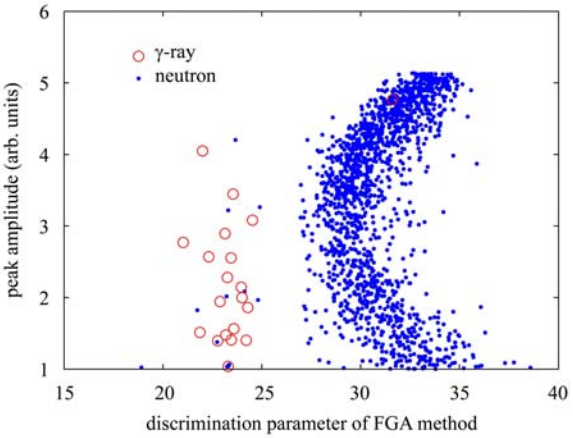

Fig. 2. A scatter plot of peak amplitude against the discrimination parameter of the FGA method applied to 774 neutron and γ-ray pulses.

3.1.3 The CC method

Different energy states are filled according to the particle interacting in the scintillator, resulting in varying de-excitation signal lifetimes. In general, a light pulse is composed of fast and slow components. The CC method used to accomplish PSD implies essentially the determination of the relative weight of the amounts of light emitted respectively in the fast and slow component of the light pulse. The implementation of the method generally relies upon the integration of the pulse over two different time intervals (Δt_{S} and Δt_{F}) corresponding to the slow and fast components, whose choice depends on the actual experimental setup. The value of the ratio $R=Q_{\text{S}}/Q_{\text{F}}$ (Q_{S} and Q_{F} are the charges in the two intervals Δt_{S} and Δt_{F}) indicates whether a neutron or a γ-ray event has taken place. If two equal amplitude neutron and γ-ray pulses are considered, the neutron pulse has a larger slow component which results in a larger R [22]. In this research, the same 774 pulses pre-identified

by using the TOF technique were applied to the CC method to test its feasibility under the 8-bit sampling condition. The integration was performed starting at the time of the peak value of each pulse and the two integrating time intervals selected were $\Delta t_{\rm S}$=100 ns and $\Delta t_{\rm F}$=20 ns.

Like the FGA method, two regions are observed in Fig. 3 by plotting the peak amplitude versus the ratio of 100 ns: 20 ns integration values of the CC method. It is clear that the right region corresponds to neutrons and the left region corresponds to γ rays in the CC method. The discrimination results of the CC method are presented in Table 1 together with TOF and FGA.

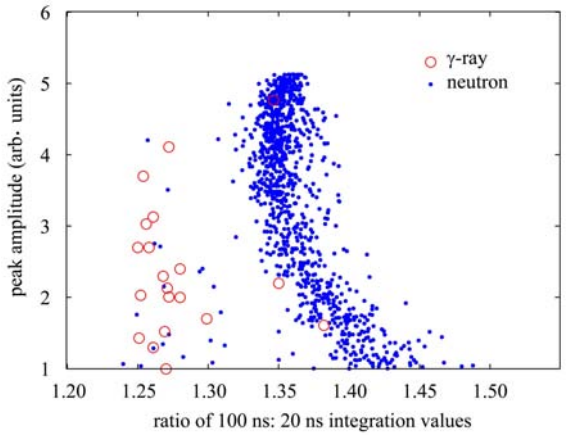

Fig. 3. A scatter plot of the peak amplitude against the ratio of 100 ns: 20 ns integration values of CC method are applied to 774 neutron and γ-ray pulses.

As shown in Table 1, the discrimination results of FGA and CC are basically consistent with those of TOF, while the results of FGA show a higher similarity to those of TOF. For instance, the total number of neutron events arising from TOF, FGA and CC are 754, 743 and 735, respectively. There are 19 neutron events mistakenly classified as γ-ray events by CC, whereas there are only 11 neutron events mistakenly classified as neutron events by FGA. It has been verified that both the FGA and CC methods are feasible under an 8-bit sampling condition while FGA has a higher degree of accuracy than CC.

3.2 Performance comparison between FGA and CC

In Section 3.1, we have certified the feasibility of CC and FGA in the environment of an 8-bit sampling system. However, there are some scatter events whose radiation type can not be identified by TOF. Because both FGA and CC are essentially PSD methods which only require the differences of the pulse shape to accomplish n-γ discrimination, they can be used to distinguish the scatter events into two classes, i.e. neutrons and γ rays. In order to further evaluate the overall n-γ separation performance of CC and FGA, two groups of pulses including some pulses induced by scatter events are applied to CC and FGA respectively to obtain FOM in this section.

3.2.1 An introduction to FOM

FOM is a current measure of the separation that can be achieved between different types of event distributions and is defined as,

$$\mathrm{FOM}=\frac{S}{\mathrm{FWHM}_{\gamma}+\mathrm{FWHM}_{\rm n}}, \tag{3}$$

where S is the separation between the centroids of the neutron peak and the γ-ray peak in the spectrum, FWHM_{γ} is the full width at half maximum (FWHM) of the spread of events classified as γ-ray events and $\mathrm{FWHM}_{\rm n}$ is the FWHM of the spread in the neutron peak [23]. If the probability distribution function of each event is consistent with the Gaussian distribution, Eq. (3) becomes:

$$\mathrm{FOM}=\frac{|\mu_{\rm n}-\mu_{\gamma}|}{2.35(\sigma_{\gamma}+\sigma_{\rm n})}, \tag{4}$$

where μ_{γ} and $\mu_{\rm n}$ are the means of the γ-ray and neutron Gaussians, respectively. The standard deviation, σ, is given as σ_{γ} and $\sigma_{\rm n}$ for the γ-ray and neutron Gaussians [18].

3.2.2 The comparison results

Group 1 comprises 679 pulses whose peak amplitudes are under 3, including 18 γ-ray pulses, 336 neutron pulses pre-identified by the TOF technique and 325 pulses induced by scatter events. Group 2 consists of 785 pulses whose peak amplitudes are above 3, including 5 γ-ray pulses, 428 neutron pulses pre-identified by using the TOF technique and 352 pulses induced by scatter events. By applying the FGA and CC methods to the pulses in Group 1 and Group 2 respectively, the scatter plots of the FGA and CC methods shown in Fig. 4(a, c) and Fig. 5(a, c) can be obtained in the same way as Fig. 2 and Fig. 3.

Based on the discrimination rules described in Section 3.1, the results of FGA and CC are derived from Fig. 4(a, c) and Fig. 5(a, c) and presented in Table 2.

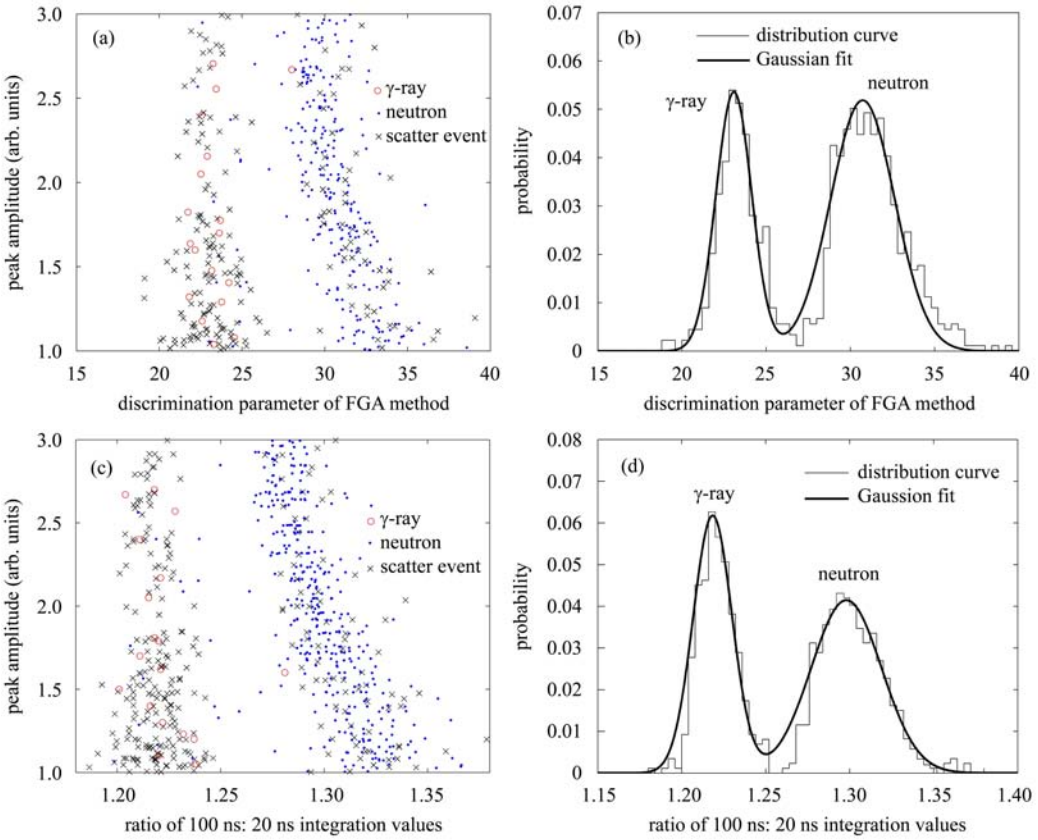

Fig. 4. (a) Scatter plot of the peak amplitude against the discrimination parameter of FGA method applied to pulses in Group 1; (b) the corresponding probability distribution histogram for the FGA data with fitted Gaussian distributions; (c) Scatter plot of the peak amplitude against the ratio of 100 ns: 20 ns integration values of CC method applied to pulses in Group 1; (d) the corresponding probability distribution histogram for the CC data with fitted Gaussian distributions.

Table 2. The neutron and γ-ray counts and estimated neutron/γ ratio derived from the scatter plots shown in Fig. 4(a, c) and Fig. 5(a, c).

data	method	$N_{\rm n}$	N_γ	$R_{\rm n/\gamma}$	$\Delta R_{\rm n/\gamma}$
Group 1	FGA	365	314	1.162	0.089
	CC	386	293	1.317	0.102
Group 2	FGA	598	187	3.198	0.268
	CC	609	176	3.460	0.296

$N_{\rm n}$ and N_γ represent the neutron and γ-ray count, respectively. $R_{\rm n/\gamma}$ is the ratio between the two counts and $\Delta R_{\rm n/\gamma}$ is the uncertainty of this ratio. It can be seen in Table 2 that for FGA the uncertainty of the ratio is smaller than that of CC. These data are normalized to the total number of pulses in the data set and are presented as probability distribution histograms in Fig. 4(b, d) and Fig. 5(b, d). Two peaks evidently correspond to the γ-ray and neutron events. With the purpose of calculating FOM, Gaussian fits have been applied to these probability distributions with the curve fitting tool available in MATLAB®.

The sum of Gaussian distribution is expressed as:

$$f(x) = A_\gamma \exp\left[-\frac{(x-\mu_\gamma)^2}{2\sigma_\gamma^2}\right] + A_{\rm n}\exp\left[-\frac{(x-\mu_{\rm n})^2}{2\sigma_{\rm n}^2}\right], \quad (5)$$

where μ_γ, $\mu_{\rm n}$, σ_γ and $\sigma_{\rm n}$ are the same as those in Eq. (4). The Gaussian functions are scaled using A_γ for the γ-ray Gaussian and $A_{\rm n}$ for the neutron Gaussian. Table 3 presents the means, standard deviations for the Gaussian fits to the experimental data shown in Fig. 4(b, d) and Fig. 5(b, d). As can be seen in these figures, there is a good fit between the Gaussian distribution and the probability distribution function, so Eq. (4) is used to calculate the FOM of each method. Substituting the variables in Eq. (4) with the corresponding data shown in Table 3, the FOMs of FGA and CC in Group 1 are calculated as: $\rm FOM_{FGA}$=1.099, $\rm FOM_{CC}$=0.929. For Group 2, the FOMs are: $\rm FOM_{FGA}$=1.146, $\rm FOM_{CC}$=1.161. For Group 1, the FOM of FGA is about 18.3 percent

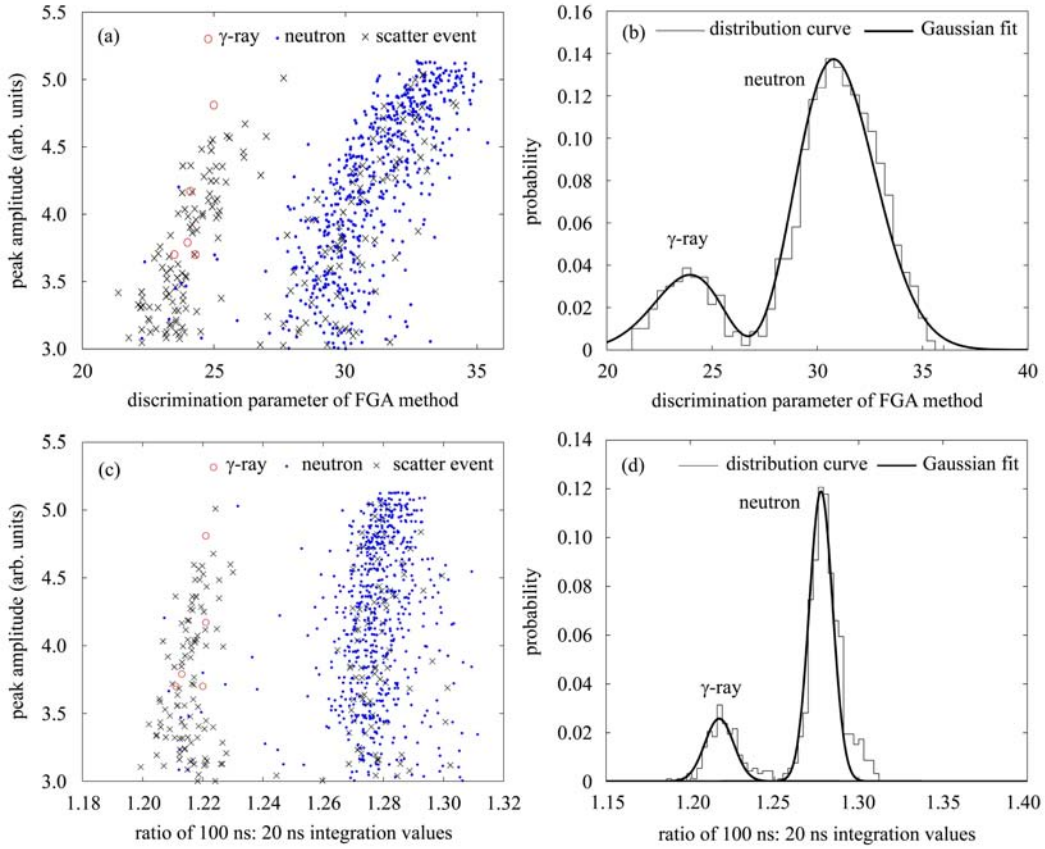

Fig. 5. (a) Scatter plot of the peak amplitude against the discrimination parameter of FGA method applied to pulses in Group 2; (b) the corresponding probability distribution histogram for the FGA data with fitted Gaussian distributions; (c) Scatter plot of the peak amplitude against the ratio of 100 ns : 20 ns integration values of CC method applied to pulses in Group 2; (d) the corresponding probability distribution histogram for the CC data with fitted Gaussian distributions.

Table 3. The values of parameters in Eq. (5) calculated from the experimental results of CC and FGA.

data	method	μ_γ	σ_γ	μ_n	σ_n
Group 1	FGA	23.080±0.140	1.499±0.189	30.730±0.190	2.690±0.210
	CC	1.227±0.001	0.016±0.001	1.298±0.001	0.030±0.002
Group 2	FGA	23.130±0.130	1.514±0.199	30.670±0.140	2.418±0.192
	CC	1.224±0.001	0.016±0.002	1.278±0.001	0.012±0.001

larger than that of CC, which indicates an improvement of the performance over CC in discriminating those neutrons and γ-rays with small pulse amplitudes. However, the FOM of CC is only approximately 1.3 percent larger than that of FGA, which shows that the performance of FGA and CC are comparable to each other when discriminating those neutrons and γ-rays with large pulse amplitudes.

4 Conclusion

The performance of the FGA method to discriminate neutrons and γ rays in the system comprising of a 14.1 MeV neutron generator, a BC501A liquid scintillator and a 5 G sample/s 8-bit oscilloscope has been investigated experimentally in detail. Firstly, the FGA and CC method are applied to the events pre-identified by TOF to accomplish n-γ discrimination. As shown in Table 1, both the FGA and CC methods are feasible in discriminating the data acquired with an 8-bit sampling system while the error on the results of FGA is smaller than that of CC. Secondly, the FOMs of FGA and CC are calculated and compared with each other. The results indicate that the performance of FGA is better than that of CC in discriminating those neutrons and γ-rays with small pulse amplitudes, which is verified by an

improvement in FOM in Group 1. Since the pulses are sampled with an 8-bit sampling system, the signal-to-noise ratio (SNR) of the pulses is low. For pulses with small amplitudes, the noise and variations of the pulse shapes are more notable. It is because FGA only exploits the frequency-domain features of the acquired pulses that it exhibits a strong insensitivity to noise and can be used to discriminate neutrons from γ rays with small pulse amplitudes.

For those n-γ discrimination methods which were originally implemented in analogue electronics, such as the CC method, their direct transpositions into the digital domain fail to exploit the intrinsic benefits of the digital domain and rarely result in program flows that are optimized to ensure speed or efficient use of memory. Besides, the main drawback of these methods is that they often require the trial-and-error setting of a certain threshold; one of the best examples is the integration time interval in the CC method. With the rapid development of related digital devices such as digital signal processors (DSP), field programmable gate arrays (FPGA) and other processors, a wide variety of digital PSD methods have recently been developed. However, most of these methods are time-domain PSD methods which use sample amplitudes of the signal at a specific time or ratio with respect to the peak amplitude. As a result, their discrimination results are very sensitive to noise and variations of the light intensity.

However, the FGA method can be used to discriminate neutrons from γ rays even in an 8-bit sampling system, which has been well proved by the research carried out in this paper. It shows that the reduction of the ADC bit resolution does not lead to the obvious deterioration of n-γ discrimination performance of FGA. Moreover, the FGA method only exploits the difference between the zero-frequency component and the first frequency component of Fourier transform of the acquired signal, which means that the burden of calculation is not heavy for FGA compared with the other digital-based discrimination methods. Based on the theoretical analysis and experimental results in this paper, it can be concluded that the FGA method has the capacity to become a promising n-γ discrimination method to be implemented in current embedded electronics systems at relatively low cost to provide real-time discrimination in many potential industrial applications.

We would like to acknowledge the support of the Institute of Nuclear Physics and Chemistry, the Chinese Academy of Engineering Physics, Mianyang, China. We also appreciate the help and advice of Dr. Li An and Dr. Pu Zheng and the technical team at the Chinese Academy of Engineering Physics, Mianyang, China.

References

1 Knoll G F. Radiation Detection and Measurement. third edition. New York: Wiley, 2000
2 Brooks F D. Nucl. Instrum. Methods, 1959, **4**: 151–163
3 Adams J M, White G. Nucl. Instrum. Methods, 1978, **156**: 459–476
4 Alexander T K, Goulding F S. Nucl. Instrum. Methods, 1961, **13**: 244–246
5 Roush M, Wilson M A, Hornyak W F et al. Nucl. Instrum. Methods, 1964, **31**: 112–114
6 Moszyński M, Costa G J, Guillaume G. Nucl. Instrum. Methods A, 1994, **350**: 226–234
7 Jastaniah S D, Sellin P J. Nucl. Instrum. Methods A, 2004, **517**: 202–210
8 Cerný J, Doležal Z, Ivanov M P et al. Nucl. Instrum. Methods A, 2004, **527**: 512–518
9 Kornilov N V, Khriatchkov V A, Dunaev M et al. Nucl. Instrum. Methods A, 2003, **497**: 467–478
10 Marrone S, Cano-Ott D, Colonna N, Domingo C et al. Nucl. Instrum. Methods A, 2002, **490**: 299–307
11 Mellow B D', Aspinall M D, Mackin R O et al. Nucl. Instrum. Methods A, 2007, **578**: 191–197
12 Aspinall M D, Mellow B D', Mackin R O et al. Nucl. Instrum. Methods A, 2007, **583**: 432–438
13 Joyce M J, Aspinall M D, Cave F D et al. IEEE Trans. Nucl. Sci., 2010, **57**: 2625–2630
14 LIU G, Aspinall M D, MA X et al. Nucl. Nucl. Instrum. Methods A, 2009, **607**: 620–628
15 Savran D, Loher B, Miklavec M et al. Nucl. Instrum. Methods A, 2010, **624**: 675–683
16 Yousefi S, Lucchese L, Aspinall M D. Nucl. Instrum. Methods A, 2009, **598**: 551–555
17 Shippen D I, Joyce M J, Aspinall M D. IEEE Trans. Nucl. Sci., 2010, **57**: 2617–2625
18 LIU G, Joyce M J, MA X et al. IEEE Trans. Nucl. Sci., 2010, **57**: 1682–1691
19 Söderström P.-A, Nyberg J, Wolters R et al. Nucl. Instrum. Methods A, 2008, **594**: 79–89
20 http://www.analog.com/en/analog-to-digital-converters/ad-converters/
21 Spencer D F, Cole J, Drigert M et al. Nucl. Instrum. Methods A, 2006, **556**: 291–295
22 Kaschuck Y, Esposito B. Nucl. Instrum. Methods A, 2005, **551**: 420–428
23 Winyard R A, Lukin J E, McBeth B W et al. Nucl. Instrum. Methods, 1971, **95**: 141–153